Exchange-Driven Spin Relaxation in Ferromagnet-Oxide-Semiconductor Heterostructures

Yu-Sheng Ou,[1] Yi-Hsin Chiu,[1] N. J. Harmon,[2] Patrick Odenthal,[3] Matthew Sheffield,[1] Michael Chilcote,[1] R. K. Kawakami,[1,3] M. E. Flatté,[2] and E. Johnston-Halperin[1,*]

[1]Department of Physics, The Ohio State University, Columbus, Ohio 43210-1117, USA

[2]Department of Physics and Astronomy, The University of Iowa, Iowa City, Iowa 52242-1479, USA

[3]Department of Physics and Astronomy, University of California, Riverside, California 92521, USA

(Received 15 July 2015; revised manuscript received 26 October 2015; published 8 March 2016)

We demonstrate that electron spin relaxation in GaAs in the proximity of a Fe/MgO layer is dominated by interaction with an exchange-driven hyperfine field at temperatures below 60 K. Temperature-dependent spin-resolved optical pump-probe spectroscopy reveals a strong correlation of the electron spin relaxation with carrier freeze-out, in quantitative agreement with a theoretical interpretation that at low temperatures the free-carrier spin lifetime is dominated by inhomogeneity in the local hyperfine field due to carrier localization. As the regime of large nuclear inhomogeneity is accessible in these heterostructures for magnetic fields <3 kG, inferences from this result resolve a long-standing and contentious dispute concerning the origin of spin relaxation in GaAs at low temperature when a magnetic field is present. Further, this improved fundamental understanding clarifies the importance of future experiments probing the time-dependent exchange interaction at a ferromagnet-semiconductor interface and its consequences for spin dissipation and transport during spin pumping.

DOI: 10.1103/PhysRevLett.116.107201

Gallium arsenide has a long history as a canonical test bed for the investigation of fundamental spin relaxation properties [1–3] and the development of prototype spintronic structures based on ferromagnet (FM)/GaAs heterostructures [4–6]. However, despite its long history, there remain significant questions regarding the fundamental spin relaxation or dissipation processes in the GaAs spin channel itself. Specifically, spin-phonon coupling [7], energy dependence of the Landé g tensor [8], and inhomogeneities in the hyperfine interaction [9] have all been proposed to explain the low-temperature (<50 K) spin relaxation in the presence of an applied magnetic field. This uncertainty hampers the use of GaAs based heterostructures to explore emerging areas of current interest, such as ferromagnetic resonance (FMR) [10–13] and thermally driven spin injection processes [14–18]. Indeed, the ability of ultrafast pump-probe spectroscopies to probe GaAs spin dynamics directly in the time domain [2] should allow for a direct measurement of the dynamic exchange coupling and dissipation that drive these phenomena if there were a fuller understanding of the interactions within GaAs.

Here our systematic investigation of the free-carrier spin lifetime in Fe/MgO/GaAs heterostructures and bare GaAs films identifies inhomogeneities in the hyperfine interaction due to the random distribution of Si donors, a mechanism introduced in Ref. [9] for bare GaAs, as the mechanism dominating the spin relaxation rate in FM/GaAs heterostructures at temperatures below 60 K. The enhanced nuclear polarization generated by scattering from the Fe/MgO interface allows us to access large effective nuclear fields in the GaAs due to the exchange-driven hyperfine coupling at low applied field (<3 kG). Comparable nuclear fields in bare GaAs require applied fields on the order of 10s of kG. This ability to enhance the nuclear field using exchange coupling, in addition to revealing the dominant source of electron spin relaxation in FM/GaAs heterostructures, allows us to infer the more complex, but still critical, consequences of these inhomogeneous nuclear fields on spin relaxation in bare GaAs films. Thus we resolve a long-standing and contentious debate about the spin lifetime's origin in GaAs at low temperature when a magnetic field is present. This more complete understanding in turn produces the quantitative description of the dynamic, exchange mediated, electron-nuclear interactions in our FM/GaAs nanostructures that is required for clear interpretations of spin pumping and other dynamic measurements involving this interface.

Our theory of the inhomogeneous hyperfine interaction is depicted in the left panel of Fig. 1(a). Large nuclear fields are induced by the process of dynamic nuclear polarization [1] from a non-equilibrium electron spin polarization generated via a combination of optical excitation and exchange coupling to the proximal FM. Since the electron-nuclear spin transfer is most efficient in the vicinity of neutral Si donors (green circles), the magnitudes of the nuclear fields (red arrows) within the GaAs are strongly inhomogeneous due to carrier localization (yellow circles). Transitions between adjacent field environments cause transverse spin relaxation [9].

The schematic structure of the samples studied in this work is shown in Fig. 1(b), with the layer thicknesses: 8 nm MgO/10 nm Fe/0.2 nm MgO/120 nm Si-doped n-type GaAs ($7 \times 10^{16}/\mathrm{cm}^3$)/400 nm $In_{0.5}Ga_{0.5}P$/n^+-type GaAs

 © 2016 American Physical Society

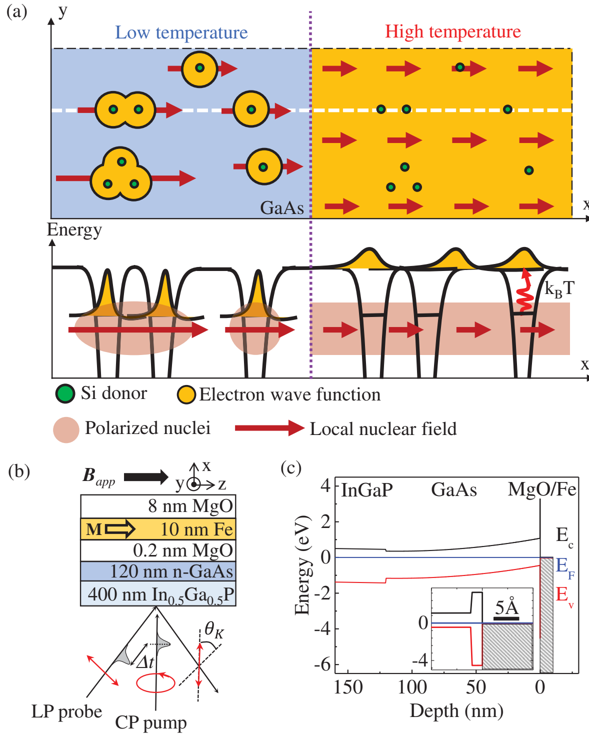

FIG. 1. (a) Top left panel: the spatial distribution of silicon donors and the inhomogeneous nuclear field resulting from electron spins trapped at the donor sites which hyperpolarize the surrounding nuclei at low temperature, as shown in the bottom left panel, which is the schematic potential profile along the white dashed line. The depth of the silicon donors has been exaggerated for clarity. Top right panel: a homogeneous nuclear field distribution at high temperature due to the delocalization of trapped carriers (bottom right panel). (b) Schematic of sample structure and time-resolved Kerr rotation (TRKR) measurement geometry. (c) Simulated band structure for the sample in (b). Inset: calculated band structure near the GaAs/MgO/Fe interface showing that the Fermi level is pinned at 0.3 eV above the GaAs valence band maximum.

(100) substrate. These samples were synthesized according to Ref. [19] with the thickness of the MgO layer optimized to maximize the exchange coupling at the Fe/GaAs interface [19] and the sample quality ensured by *in situ* reflection high-energy electron diffraction (RHEED) and atomic force microscopy (AFM). Figure 1(c) shows the simulated band structure of the sample calculated using a self-consistent one-dimensional Schrödinger-Poisson solver (BandEng). The band offset at the interface [Fig. 1(c), inset] is determined by previous studies using x-ray and ultraviolet photoelectron spectroscopies to study the band structure of the Fe/MgO/GaAs tunnel junction [20]. A control sample is grown with a similar structure but without the Fe/MgO layer, and both samples are mounted face down on 100 μm thick sapphire wafers so that the n^+-type GaAs substrates can be removed by selective wet etching using the $In_{0.5}Ga_{0.5}P$ layer as a chemically selective etch stop [21].

We establish a baseline for the evaluation of the quality of our heterostructures by probing the strength of the interfacial exchange interaction in these heterostructures via time-resolved Kerr rotation (TRKR) [19,22,23]. A schematic of the technique is shown in Fig. 1(b); a circularly polarized (CP) pump pulse excites electron spins in GaAs along its propagation direction, which then precess in the presence of a transverse magnetic field ($\boldsymbol{B}_{tot} = B_{tot}\hat{z}$). After a time delay Δt, the Kerr rotation (θ_K) of a much weaker linearly polarized (LP) probe pulse measures the spin component along its propagation direction. The time dependence of the Kerr angle can be described by the following equation [24]:

$$\theta_K(\Delta t) = \theta_0(e^{-(\Delta t/T_2^*)} + N_0 e^{-(\Delta t/T_h)})\cos(\omega_L \Delta t + \phi), \quad (1)$$

where θ_0 is the maximal Kerr angle and N_0 is the ratio of photoexcited to equilibrium electrons at $\Delta t = 0$, T_2^* is the ensemble transverse electron spin relaxation time, T_h is the hole carrier recombination time, $\omega_L = g\mu_B B_{tot}/\hbar$ is the Larmor precession frequency due to both applied field ($\boldsymbol{B}_{app} = B_{app}\hat{z}$) and local field ($\boldsymbol{B}_{loc} = B_{loc}\hat{z}$) $\boldsymbol{B}_{tot} = \boldsymbol{B}_{app} + \boldsymbol{B}_{loc}$, and ϕ is the phase of the spin precession. The two exponential terms reflect the fact that the photoexcited holes, while not directly detected due to their rapid spin relaxation, do act to dephase the electron ensemble through the Bir-Aranov-Pikus mechanism until they recombine (typically in less than 100 ps [25]).

The TRKR time scans for both the Fe/MgO/GaAs heterostructure and the GaAs control are shown in Fig. 2(a). Laser pulses of 130-fs duration and 76 MHz repetition rate are generated by a mode-locked Ti:sapphire laser, and are split into pump and probe pulse trains whose power ratio is ~7, with a time-averaged pump power density of 119 W/cm^2. The clear difference in ω_L (or, equivalently, B_{tot}) between the Fe/MgO/GaAs and GaAs structures implies a variance in B_{loc} between the two samples (roughly -2 and $+0.2$ kG, respectively). The magnitude and sign of B_{loc} in Fe/MgO/GaAs has been attributed to a hyperpolarization of the Ga and As nuclei [22,23] in the proximity of the ferromagnetic layer [ferromagnetic proximity polarization (FPP)], and is consistent with previous FPP measurements.

Figure 2(b) shows a schematic diagram detailing the fundamental interactions underlying the FPP effect. We consider separately free-carrier spins that reflect from the Fe/MgO layer [26] and spins that evolve purely within the GaAs. The former will acquire a net orientation parallel to the magnetization of the Fe layer through the interfacial exchange interaction, i.e., the FPP process [19,22,23] $\boldsymbol{S}_{FPP}$, while the latter will relax antiparallel to the applied field $\boldsymbol{S}_{rel}$ (the Landé g factor in GaAs is -0.44 [27]). These two nonequilibrium electron spin populations both act to dynamically polarize nuclear spins ($\boldsymbol{I}$) via the hyperfine interaction, and the polarized nuclear spins in turn create an effective local field $\boldsymbol{B}_n^{tot} = B_n^{tot}\hat{z}$ acting on the photoexcited spins. This analysis identifies the local magnetic field measured by the Larmor precession shown in Fig. 2(a), B_{loc}, as arising from an effective nuclear field B_n^{tot} due to the optically induced nonequilibrium nuclear polarization. Further evidence for the nuclear origin of B_{loc} can be found

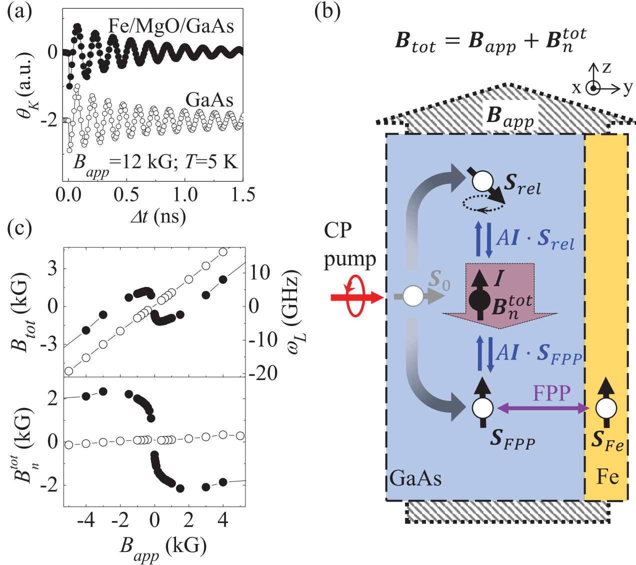

FIG. 2. (a) Measured Kerr rotation (θ_K) vs Δt for a Fe/MgO/GaAs heterostructure (solid circles) and a control GaAs epilayer (open circles) at $T = 5$ K and $B_{app} = 12$ kG. The data are offset for clarity. (b) A cartoon illustrates that a nuclear field antiparallel to the applied field in a Fe/MgO/GaAs heterostructure results from the hyperfine coupling between GaAs nuclear spins ($\boldsymbol{I}$), and two nonequilibrium spin populations, $\boldsymbol{S}_{rel}$ and $\boldsymbol{S}_{FPP}$ (see text). (c) Top panel: total field $B_{\rm tot}$ (Larmor frequency ω_L) as a function of B_{app} between -5 and $+5$ kG for Fe/MgO/GaAs and bare GaAs at $T = 5$ K. Bottom panel: nuclear field B_n^{tot} ($B_n^{tot} = B_{tot} - B_{app}$) as a function of B_{app}.

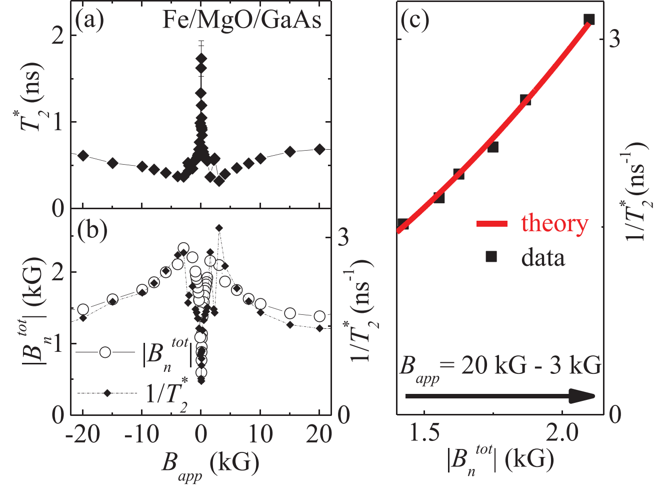

FIG. 3. (a) Spin relaxation time (T_2^*, solid diamonds) and (b) $|B_n^{tot}|$ (open circles) and $1/T_2^*$ (solid diamonds) as a function of B_{app} for Fe/MgO/GaAs up to 20 kG at $T = 5$ K. (c) $1/T_2^*$ as a function of $|B_n^{tot}|$. Solid squares represent experimental data and the red line represents a quantitative fit using the model presented in Ref. [9] (see main text and Ref. [28]).

in the resonant suppression of B_{loc} at the various nuclear magnetic resonance (NMR) frequencies of the Ga and As nuclei [28–30]. The observation of $B_n^{tot} = -2$ kG in Fe/MgO/GaAs indicates that $\boldsymbol{B}_n^{tot}$ is dominated by $\boldsymbol{S}_{FPP}$, while the fact that $B_n^{tot} = +0.2$ kG in the GaAs control indicates that the nuclear polarization arises from $\boldsymbol{S}_{rel}$.

Although the magnitude and sign of B_n^{tot} in Fe/MgO/GaAs is a strong indication of FPP, more compelling evidence is the ferromagnetic imprinting of the nuclear spin polarization [22,23]. As can be seen in Fig. 2(c) the dependence of B_{tot} on B_{app} (top panel) has both a linear component (from the Zeeman dependence on B_{app}) and a component that tracks with the magnetization of the Fe layer, switching at fields below the experimental resolution (~0.02 kG) and saturating at $B_{app} \sim \pm 3$ kG. This behavior is more clearly seen in the bottom panel of Fig. 2(c) where the linear Zeeman dependence has been subtracted. This is in contrast to the behavior in the GaAs control, where B_{tot} (ω_L) and B_n^{tot} scale linearly with B_{app} (open circles) [1,31,32]. These results are both quantitatively and qualitatively consistent with previous studies [22,23], and confirm the high interfacial quality of the sample.

We now move beyond previous work to consider the impact of this interfacial exchange coupling and consequent nuclear polarization on the spin relaxation or dissipation in the GaAs layer. Figures 3(a) and 3(b) show T_2^* and the magnitude of B_n^{tot} ($|B_n^{tot}|$) as a function of applied field B_{app}, respectively. A remarkable correlation is evident, with $|B_n^{tot}| \sim 1/T_2^*$. There are two distinct regimes evident in these measurements. First, for B_{app} below 0.5 kG there is a strong enhancement of T_2^* and concurrent suppression of $|B_n^{tot}|$. This is a well-known effect arising from the nuclear depolarization driven by the nuclear dipole-dipole coupling [1,31]. Second, for fields above 0.5 kG we observe a previously undocumented field dependence that appears to arise from a competition between the nuclear field generated by the FPP effect and by Zeeman splitting, $\boldsymbol{B}_n^{FPP}$ and $\boldsymbol{B}_n^{Z}$, respectively. As can be seen in Fig. 2(c), with increasing B_{app} the FPP-driven polarization is initially much larger than the Zeeman-driven polarization, but saturates as the magnetization saturates at $B_{app} \sim 3$ kG. In contrast, the Zeeman-driven polarization grows slowly but continuously, increasing linearly for the entire field range studied here. Since these two contributions have opposite sign (Fig. 2), their competition gives rise to an inflection point in the total nuclear field, $B_n^{tot} = B_n^{FPP} + B_n^{Z}$, as can be seen in the maximum in $|B_n^{tot}|$ in Fig. 3(b).

In general, this correspondence between $|B_n^{tot}|$ and T_2^*, which has not been previously observed nor understood, strongly indicates that the dominant spin relaxation in this regime is via hyperfine coupling. To gain insight into the origin of this hyperfine-dominated spin relaxation, we consider a theory in which the inhomogeneous nuclear field is due to the nonuniform donor distribution in the GaAs [Fig. 1(a)], leading to inhomogeneous dephasing of the photoexcited electron spins [9]. In this theory, $\boldsymbol{S}_{FPP}$ and $\boldsymbol{S}_{rel}$ can both relax into donor-bound localized states surrounding the Si dopants in the GaAs as shown in the left panel of Fig. 1(a). These trapped spins can either directly hyperpolarize nuclei within their Bohr radius (path 1) or polarize donor electrons via the exchange interaction [1,33] that then hyperpolarize surrounding nuclei (path 2), resulting in a

puddle of hyperpolarized nuclear spin oriented either parallel (FPP) or antiparallel (Zeeman) to B_{app}. These randomly located polarized nuclei in turn give rise to an inhomogeneous nuclear field distribution that leads to the dephasing of itinerant photoexcited carriers that move across those donor sites. The spin relaxation via path 1 can be calculated using a theory of continuous-time random walk for spin [34,35]. As was recently shown in Ref. [9], in the motional narrowing limit the existence of the nuclear field inhomogeneity gives rise to an anisotropic spin relaxation term, $1/T_2^* \sim (B_n^{tot})^2$. A quantitative fit of this theory to the measured values of $1/T_2^*$ for B_{app} from 20 kG–3 kG is shown in Fig. 3(c), demonstrating remarkably good agreement and yielding a characteristic rate for diffusing between local nuclear environments of 178 ps. In contrast, the spin-phonon coupling model presented in Ref. [7] provides a quantitative estimate of $1/T_2^*$ that differs from experiment by 5 orders of magnitude [28].

Critically, this theory makes two implicit predictions about the expected behavior of T_2^* as a function of the temperature of the sample T, and B_{app}. Considering first the effect of the sample temperature, we note that raising the system temperature should weaken the hyperfine coupling due to the thermal activation of localized carriers [1]. This in turn should lead to a more homogeneous nuclear field as well as an overall decrease in $|B_n^{tot}|$ as thermal depolarization of the nuclear bath competes with dynamic nuclear polarization as shown in the right panel of Fig. 1(a). This decrease in inhomogeneity in the nuclear field should, in principle, lead to an enhancement of T_2^*.

These trends are clearly observed in the temperature-dependent data presented in Figs. 4(a) and 4(b) for $|B_n^{tot}|$ and T_2^*, respectively. Considering first data taken for $B_{app} =$ 0.18 kG (black circles) and at temperatures below 40 K, we see a monotonic decrease in $|B_n^{tot}|$ and a monotonic increase in T_2^* for increasing temperature. For temperatures above 40 K, the trend in $|B_n^{tot}|$ continues to monotonically decrease but the increase in T_2^* shows a local maximum, with T_2^* decreasing for higher temperatures. This behavior is qualitatively consistent with a continuous decrease in the strength of hyperfine-induced dephasing of the spin ensemble until it is no longer the dominant spin relaxation mechanism and is quantitatively consistent with the temperature scale for the thermal ionization of the Si dopants (full ionization is expected at roughly 69 K [36]). Comparison of the high-temperature behavior of T_2^* with previous reports in bare GaAs [2] suggests that the high-temperature regime is dominated by D'yakonov-Perel (DP) spin relaxation [2,7] (dashed black line).

We note that this nonmonotonic temperature dependence of T_2^* was also observed in bare GaAs, but at much higher B_{app}(>10 kG) [2,37]. This difference in field scale is inconsistent with the recent prediction that spin-phonon coupling is the dominant spin relaxation pathway at low temperature in the presence of a significant B_{app} [7]. The derived spin relaxation rate based on the spin-phonon coupling model is proportional to $(B_{app})^2$ at a fixed

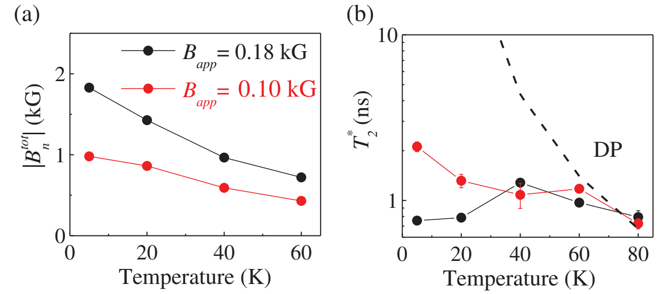

FIG. 4. (a) $|B_n^{tot}|$ and (b) T_2^* as a function of temperature for $B_{app} = 0.18$ kG (black circles) and 0.10 kG (red circles) for a Fe/MgO/GaAs heterostructure. The error bars for all points are smaller than the symbol size. The black dashed line is the DP prediction of the temperature dependence of T_2^*.

temperature, and in the low B_{app} region discussed here, the rate is too small to account for the measured magnitude of T_2^* [28]. However, while the applied field is quite different in bare GaAs [2,37,38] and FM/GaAs heterostructures, in both cases the hyperfine fields are in fact comparable [O ($\sim$1 kG)] when the peak in T_2^* is observed. This clearly identifies the peak in T_2^* as the outcome of competition between two spin relaxation mechanisms, inhomogeneous hyperfine interactions [9] and D'yakonov-Perel spin relaxation, in both systems. This identification is further supported by the comparison of $|B_n^{tot}|$ and T_2^* in bare GaAs epilayers [28], revealing an inverse correlation similar to the data presented in Fig. 3.

The second, correlated, prediction of our model is that suppressing the hyperfine coupling should cause the local maximum in T_2^* at 40 K to disappear and allow the next most dominant spin relaxation mechanism (presumably DP in these samples) to be evident at all temperatures. The data in Figs. 3(a) and 3(b) provide a path to realizing just such a measurement through the low field dipole-induced depolarization of $|B_n^{tot}|$. Reducing B_{app} from 0.18 to 0.10 kG dramatically reduces $|B_n^{tot}|$ from +2 to +1 kG at $T = 5$ K in the Fe/MgO/GaAs heterostructure, and the data in Fig. 4(a) show that this suppression persists to higher temperature. This reduction in nuclear spin polarization leads to a suppression of the local maximum in T_2^* at 40 K, and T_2^* converges toward the DP prediction across the entire measured temperature range, as predicted above. The failure to fully recover the DP prediction can be explained by the fact that the finite length of our mechanical delay line and laser repetition rate place a lower bound on the value of B_{app} for which we can experimentally resolve T_2^*. As a result, we cannot fully suppress $|B_n^{tot}|$ and therefore must measure in a regime with some residual hyperfine-driven inhomogeneity.

In conclusion, we observe a strong dependence of electron spin relaxation time on the FPP-enhanced hyperfine field in Fe/MgO/GaAs heterostructures. Our results are quantitatively consistent with a theory of spin relaxation from the effective nuclear field due to carrier localization at Si donors at low temperature, and clarify the origin of a local

maximum in the value of T_2^* as a function of temperature. Further, our results retroactively explain, for the first time, the deviation from D'yakonov-Perel spin scattering at low temperature that has been previously observed in bare GaAs films. This work establishes a comprehensive fundamental framework for understanding spin relaxation or dissipation in GaAs based ferromagnet/normal material heterostructures that may serve as the basis for coherent, time-resolved studies of spin transfer and dynamic exchange coupling in the emerging field of dynamically driven spin pumping. For example, while the current study focuses on the impact of the FPP process on the GaAs layer, symmetry argues that the exchange-driven polarization of the photocarriers in GaAs must be accompanied by a concurrent *depolarization* of the Fe layer.

This Letter is based upon work supported by the U.S. Department of Energy, Office of Science, Office of Basic Energy Sciences, under Grant No. DE-FG02-03ER46054 and by the Center for Emergent Materials: an NSF MRSEC under Grant No. DMR-1420451. The authors acknowledge John Carlin for the growth of the GaAs epitaxial layers, Mark Brenner for the deposition of the As capping layers, Kurtis Wickey for technical assistance, and the NanoSystems Laboratory at the Ohio State University.

*To whom all correspondence should be addressed.
ejh@mps.ohio-state.edu

[1] F. Meier and B. P. Zachachrenya, *Optical Orientation* (North-Holland, Amsterdam, 1984).
[2] J. M. Kikkawa and D. D. Awschalom, Phys. Rev. Lett. **80**, 4313 (1998).
[3] *Semicondoctor Spintronics and Quantum Computation*, edited by D. D. Awschalom, D. Loss, and N. Samarth (Springer Verlag, Heidelberg, 2002).
[4] R. Fiederling, M. Keim, G. Reuscher, W. Ossau, G. Schmidt, A. Waag, and L. W. Molenkamp, Nature (London) **402**, 787 (1999).
[5] Y. Ohno, D. K. Young, B. Beschoten, F. Matsukura, H. Ohno, and D. D. Awschalom, Nature (London) **402**, 790 (1999).
[6] X. Lou, C. Adelmann, S. A. Crooker, E. S. Garlid, J. Zhang, K. S. Madhukar Reddy, S. D. Flexner, C. J. Palmstrøm, and P. A. Crowell, Nat. Phys. **3**, 197 (2007).
[7] W. O. Putikka and R. Joynt, Phys. Rev. B **70**, 113201 (2004).
[8] F. X. Bronold, I. Martin, A. Saxena, and D. L. Smith, Phys. Rev. B **66**, 233206 (2002).
[9] N. J. Harmon, T. A. Peterson, C. C. Geppert, S. J. Patel, C. J. Palmstrøm, P. A. Crowell, and M. E. Flatté, Phys. Rev. B **92**, 140201(R) (2015).
[10] Y. Tserkovnyak, A. Brataas, and G. E. W. Bauer, Phys. Rev. Lett. **88**, 117601 (2002).
[11] Y. Tserkovnyak, A. Brataas, and G. E. W. Bauer, Phys. Rev. B **66**, 224403 (2002).
[12] B. Heinrich, Y. Tserkovnyak, G. Woltersdorf, A. Brataas, R. Urban, and G. E. W. Bauer, Phys. Rev. Lett. **90**, 187601 (2003).
[13] E. Saitoh, M. Ueda, H. Miyajima, and G. Tatara, Appl. Phys. Lett. **88**, 182509 (2006).
[14] K. Uchida, S. Takahashi, K. Harii, J. Ieda, W. Koshibae, K. Ando, S. Maekawa, and E. Saitoh, Nature (London) **455**, 778 (2008).
[15] K. Uchida, J. Xiao, H. Adachi, J. Ohe, S. Takahashi, J. Ieda, T. Ota, Y. Kajiwara, H. Umezawa, H. Kawai, G. E. W. Bauer, S. Maekawa, and E. Saitoh, Nat. Mater. **9**, 894 (2010).
[16] C. M. Jaworski, J. Yang, S. Mack, D. D. Awschalom, J. P. Heremans, and R. C. Myers, Nat. Mater. **9**, 898 (2010).
[17] J. Xiao, G. E. W. Bauer, K.-c. Uchida, E. Saitoh, and S. Maekawa, Phys. Rev. B **81**, 214418 (2010); **82**, 099904(E) (2010).
[18] A. Slachter, F. L. Bakker, J-P. Adam, and B. J. van Wees, Nat. Phys. **6**, 879 (2010).
[19] Y. Li, Y. Chye, Y. F. Chiang, K. Pi, W. H. Wang, J. M. Stephens, S. Mack, D. D. Awschalom, and R. K. Kawakami, Phys. Rev. Lett. **100**, 237205 (2008).
[20] Y. Lu, J. C. Le Breton, P. Turban, B. Lépine, P. Schieffer, and G. Jézéquel, Appl. Phys. Lett. **89**, 152106 (2006).
[21] H. Uchiyama, H. Ohta, T. Shiota, C. Takubo, K. Tanaka, and K. Mochizuki, J. Vac. Sci. Technol. B **24**, 664 (2006).
[22] R. K. Kawakami, Y. Kato, M. Hanson, I. Malajovich, J. M. Stephens, E. Johnston-Halperin, G. Salis, A. C. Gossard, and D. D. Awschalom, Science **294**, 131 (2001).
[23] R. J. Epstein, I. Malajovich, R. K. Kawakami, Y. Chye, M. Hanson, P. M. Petroff, A. C. Gossard, and D. D. Awschalom, Phys. Rev. B **65**, 121202 (2002).
[24] J. M. Kikkawa, I. P. Smorchkova, N. Samarth, and D. D. Awschalom, Science **277**, 1284 (1997).
[25] V. A. Sih, E. Johnston-Halperin, and D. D. Awschalom, Proc. IEEE **91**, 752 (2003).
[26] C. Ciuti, J. P. McGuire, and L. J. Sham, Phys. Rev. Lett. **89**, 156601 (2002).
[27] C. Weisbuch, C. Hermann, and G. Fishman, Dynamics of Excitonic Complexes and Detection of Electron Spin Resonance by Optical Spin Orientation Techniques, in *Proceedings of the Twelfth International Conference on the Physics of Semiconductors, Stuttgart, 1974*, edited by M. H. PiKuhn, (Vieweg+Teubner Verlag, Stuttgart, 1974), p. 761.
[28] See Supplemental Material at http://link.aps.org/supplemental/10.1103/PhysRevLett.116.107201, which includes Refs. [29,30], for control measurements and quantitative comparison with additional models.
[29] G. Salis, D. T. Fuchs, J. M. Kikkawa, D. D. Awschalom, Y. Ohno, and H. Ohno, Phys. Rev. Lett. **86**, 2677 (2001).
[30] G. Salis, D. D. Awschalom, Y. Ohno, and H. Ohno, Phys. Rev. B **64**, 195304 (2001).
[31] D. Paget, G. Lampel, B. Sapoval, and V. I. Safarov, Phys. Rev. B **15**, 5780 (1977).
[32] M. I. D'yakonov and V. I. Perel', Zh. Eksp. Teor. Fiz. **65**, 362 (1973) [Sov. Phys. JETP **38**, 177 (1974)].
[33] L. L. Buishvili, N. P. Giorgadze, and A. I. Ugulava, Fiz. Tverd. Tela **16**, 3043 (1974).
[34] N. J. Harmon and M. E. Flatté, Phys. Rev. Lett. **110**, 176602 (2013).
[35] N. J. Harmon and M. E. Flatté, Phys. Rev. B **90**, 115203 (2014).
[36] S. M. Sze, *Semiconductor Devices, Physics and Technology*, 2nd ed. (Wiley, New York, 2001).
[37] P. E. Hohage, G. Bacher, D. Reuter, and A. D. Wieck, Appl. Phys. Lett. **89**, 231101 (2006).
[38] J. M. Kikkawa and D. D. Awschalom, Science **287**, 473 (2000).